HHS Public Access

Author manuscript

Mol Microbiol. Author manuscript; available in PMC 2017 January 01.

Published in final edited form as:

Mol Microbiol. 2016 January ; 99(2): 254–273. doi:10.1111/mmi.13230.

Diverse mechanisms of post-transcriptional repression by the small RNA regulator of glucose-phosphate stress

Maksym Bobrovskyy[1] and **Carin K. Vanderpool**[1,*]

[1]Department of Microbiology, University of Illinois at Urbana-Champaign, 601 S. Goodwin Ave., Urbana, IL 61801

Abstract

The *Escherichia coli* small RNA SgrS controls metabolic stress response that occurs upon accumulation of certain glycolytic intermediates. SgrS base pairs with and represses translation of *ptsG* and *manXYZ* mRNAs, which encode sugar transporters, and activates translation of *yigL* mRNA, encoding a sugar phosphatase. This study defines four new genes as direct targets of *E. coli* SgrS. These new targets, *asd*, *adiY, folE* and *purR,* encode transcription factors or enzymes of diverse metabolic pathways, including aspartate semialdehyde dehydrogenase, arginine decarboxylase gene activator, GTP cyclohydrolase I and a repressor of purine biosynthesis, respectively. SgrS represses translation of each of the four target mRNAs via distinct mechanisms. SgrS binding sites overlapping the Shine-Dalgarno sequences of *adiY* and *folE* mRNAs suggest that SgrS pairing with these targets directly occludes ribosome binding and prevents translation initiation. SgrS binding within the *purR* coding sequence recruits the RNA chaperone Hfq to directly repress *purR* translation. Two separate SgrS binding sites were found on *asd* mRNA, and both are required for full translational repression. Ectopic overexpression of *asd*, *adiY* and *folE* is specifically detrimental to cells experiencing glucose-phosphate stress, suggesting that SgrS-dependent repression of the metabolic functions encoded by these targets promotes recovery from glucose-phosphate stress.

Introduction

Small regulatory RNAs (sRNAs) are post-transcriptional regulators of gene expression found in all domains of life. Many bacterial sRNAs control large regulons and perform vital functions in cellular metabolism and physiology (Bobrovskyy and Vanderpool, 2013). Synthesis of the majority of sRNAs is tightly regulated and they are expressed under specific conditions such as iron limitation (Masse *et al.*, 2007), glucose-phosphate overload (Vanderpool and Gottesman, 2007), oxidative stress (Altuvia *et al.*, 1997) and acid stress (Opdyke *et al.*, 2004). Most bacterial sRNAs are 50 nt to 300 nt in length and base pair with mRNAs to modulate mRNA stability and translation. The Hfq protein, an RNA chaperone, stabilizes sRNAs (Sledjeski *et al.*, 2001; Moller *et al.*, 2002) and facilitates sRNA-mRNA base pairing (Moller *et al.*, 2002; Zhang *et al.*, 2002). A common mechanism for sRNA-mediated negative regulation involves occlusion of the ribosome binding site (RBS) via

*Corresponding author, Carin K. Vanderpool, Ph.D., Department of Microbiology, University of Illinois at Urbana-Champaign, C213 CLSL, MC-110, 601 S. Goodwin Ave., Urbana, IL 61801, (t) 217-333-7033, (f) 217-244-6697, cvanderp@life.illinois.edu.

interactions of the sRNA and the Shine-Dalgarno sequence in the 5′ untranslated region (UTR) of the target mRNA. Such sRNA-mRNA duplexes are typically subject to degradation by the ribonuclease RNase E and associated components of the degradosome (Masse *et al.*, 2003; Masse and Gottesman, 2002; Morita *et al.*, 2005). In a handful of cases, sRNAs do not block translation initiation but instead specifically target mRNAs for degradation by base pairing within the coding sequence (Pfeiffer *et al.*, 2009) or in an upstream region of the 5′ UTR (Desnoyers *et al.*, 2009). Positive regulation by sRNAs is less commonly described, but there are a number of examples where sRNA base pairing in a 5′ UTR prevents formation of a translation-inhibitory secondary structure (Lease *et al.*, 1998; Morfeldt *et al.*, 1995; Prevost *et al.*, 2007; Obana *et al.*, 2010) or where base pairing stabilizes target transcripts by protecting them from RNase E (Frohlich *et al.*, 2013; Papenfort *et al.*, 2013).

Sugars are important sources of carbon and energy for bacteria, yet excessive intracellular accumulation of phosphorylated sugar intermediates can be detrimental to the cell and cause growth inhibition (Englesberg *et al.*, 1962; Lee *et al.*, 2009) or death (Irani and Maitra, 1977; Yarmolinsky *et al.*, 1959; Prasad and Freese, 1974). While the physiological mechanisms responsible for growth inhibition accompanying sugar-phosphate accumulation remain unclear in many cases, recent work suggests that in some instances the accumulated sugars themselves are not the primary stressor. Rather, simultaneous depletion of other metabolites seems to result in changes in gene expression and growth inhibition (Lee *et al.*, 2009; Richards and Vanderpool, 2013; Lee *et al.*, 2014). In these cases, it is postulated that the response that alters gene regulation helps prevent or alleviate metabolite accumulation or depletion in order to restore homeostasis (Lee *et al.*, 2014; Lee *et al.*, 2009; Barupal *et al.*, 2013).

Perturbations in glycolytic flux due to mutations (Kimata *et al.*, 2001; Morita *et al.*, 2003) or uptake of non-metabolizable sugar analogs α-methylglucoside (αMG) and 2-deoxyglucose (2DG) result in sugar-phosphate accumulation and growth inhibition (Kornberg and Lambourne, 1994; Rice and Vanderpool, 2011; Vanderpool and Gottesman, 2004; Sun and Vanderpool, 2011). This condition is referred to as glucose-phosphate stress because of the association with accumulation of glucose-6-phosphate (or its analogs) (Vanderpool and Gottesman, 2004). Our previous work has demonstrated that the sRNA SgrS is crucial for the response to glucose-phosphate stress and is highly expressed under this stress condition (Vanderpool and Gottesman, 2004). SgrS is a 227-nt long sRNA conserved among γ-proteobacteria (Horler and Vanderpool, 2009). SgrS represses translation of two mRNA targets, *ptsG* and *manXYZ* (Vanderpool 2004; Kawamoto 2006; Rice 2011, 2012), encoding transporters of the phosphoenolpyruvate phosphotransferase system (PEP-PTS), $EIICB^{glc}$ (PtsG) and $EIIABCD^{man}$ (ManXYZ), respectively (Postma *et al.*, 1993; Robillard and Broos, 1999). SgrS activates a third mRNA target, *yigL*, which encodes haloacid dehalogenase (HAD)-like phosphatase that dephosphorylates sugars prior to their efflux (Papenfort *et al.*, 2013). SgrS base pairing with *yigL* mRNA protects it from RNase E-mediated degradation (Papenfort *et al.*, 2013). Together, SgrS regulation of these three mRNA targets reduces accumulation of sugar-phosphates by inhibiting synthesis of sugar transporters and enhances dephosphorylation and efflux of sugars. We have shown that while SgrS regulation of *ptsG*, *manXYZ* and *yigL* is necessary, it is not sufficient for full recovery from glucose-phosphate

stress under certain circumstances (Sun and Vanderpool, 2013). We hypothesized that SgrS regulation of other as yet undefined mRNA targets might be important for cell physiology during stress. Therefore, in order to better understand how bacteria restore metabolic homeostasis during glucose-phosphate stress and the role of SgrS in mediating this response we performed global transcriptomic analyses to identify genes differentially regulated directly by SgrS. With this work, we more than double the number of genes in the SgrS regulon by characterizing regulation of four new targets: *asd*, *adiY*, *folE* and *purR* mRNAs. While the specific function of these genes in glucose-phosphate stress remains to be uncovered, we present evidence that dysregulation of these genes specifically under stress conditions is deleterious to cell growth. This study suggests that SgrS regulation of target mRNAs not only modulates sugar uptake and efflux, but also modifies metabolism in order to promote homeostasis and growth recovery.

Results

Genes differentially regulated by ectopically expressed SgrS

Glucose-phosphate stress caused by αMG results in growth inhibition (particularly of *sgrS* mutants) and we expect that expression of many genes changes due to secondary effects from growth inhibition (data not shown). To reduce these secondary effects, SgrS was expressed ectopically in *E. coli* for 10 minutes in the absence of stress and RNA-seq analyses were performed. There is no discernible difference in growth of SgrS-expressing cells compared to vector control cells under these conditions (data not shown). The gene expression profile of cells expressing SgrS (from a P_{lac}-sgrS plasmid) was compared to that of the vector control strain (Table S1). For this experiment, genes were considered differentially expressed if they met the following criteria: >1.5-fold change in expression between samples with statistical significance of $<1\times10^{-2}$ (qValue as determined by Rockhopper) (McClure *et al.*, 2013). Only 23 genes fell within these thresholds and were selected for further analysis (Table 1).

Among the genes that were differentially expressed after the 10-minute pulse of SgrS, *ptsG*, *manX* and *yigL* were already known to be direct SgrS targets (Papenfort *et al.*, 2013; Rice and Vanderpool, 2011; Vanderpool and Gottesman, 2004). Other characterized SgrS-regulated genes *manY* and *manZ* (in an operon with *manX*) were affected, but missed the fold-change cutoff (they were downregulated 1.45-fold (qValue of 4.2×10^{-4}) and 1.41-fold (qValue of 1.37×10^{-7}), respectively (Table S1)). This was expected as maximal reduction of *manXYZ* mRNA levels occurs at a later time, more than 10 minutes after SgrS induction (Rice and Vanderpool, 2011). In addition to these known targets, a number of genes encoding diverse (or unknown) functions were differentially regulated in response to SgrS expression. These include genes involved in aspartate metabolism, purine biosynthesis, folate production and metal homeostasis (Table 1).

RT-qPCR was used to confirm expression changes for some of the candidate targets identified in RNA-seq experiments (Table 1, Table S1, Fig. S1A). Results of RT-qPCR analysis were consistent with RNA-seq for 10 out of 12 genes tested (Fig. S1A). Levels of candidate mRNA targets *asd*, *folE*, *yeeD*, *yeeE* and *purR* were decreased by ~2-fold in response to SgrS induction while levels of *cusC* mRNA decreased >10-fold (Fig. S1A). SgrS

induction resulted in increased levels of *ykgM* and *znuA* mRNAs (Fig. S1A), which was consistent with RNA-seq results (Table 1). The *nepI* mRNA (encoding a purine ribonucleoside efflux transporter) showed ~3-fold reduced levels in response to SgrS induction via RT-qPCR, whereas very little difference was observed in RNA-seq (Fig. S1A, Table S1). Regulation of *ydjN* was inconsistent with RNA-seq, while *zinT* did not show differential regulation (Fig. S1A, Table 1), so both of these genes were excluded from further analyses.

One additional target candidate, *adiY*, was analyzed based on microarray analyses of RNA from strains grown under the same conditions as for RNA-seq experiments (J. B. Rice and C. K. Vanderpool, unpublished). The *adiY* gene encodes a transcription factor regulating arginine decarboxylase genes. Expression of *adiY* is highest under anaerobic and low pH conditions (Stim-Herndon *et al.*, 1996). While strains for microarray and RNA-seq analyses were grown aerobically, perhaps slight differences in growth conditions led to detection of *adiY* mRNA in microarrays, but not RNA-seq. Regardless, to further test whether *adiY* mRNA is regulated by SgrS, cultures were grown without aeration to allow for sufficient *adiY* expression for detection by qRT-PCR. In cultures where SgrS was induced, *adiY* mRNA levels were reduced ~5-fold compared to vector control cultures (Fig. S1B).

Identifying genes post-transcriptionally regulated by SgrS in E. coli

To further narrow the search for direct targets of SgrS, we took advantage of computational base pairing prediction programs such as CopraRNA (Wright *et al.*, 2013), IntaRNA (Busch *et al.*, 2008; Richter *et al.*, 2010) and RNAhybrid (Rehmsmeier *et al.*, 2004; Kruger and Rehmsmeier, 2006) to identify potential SgrS-mRNA interactions. Several mRNAs that were differentially regulated in RNA-seq experiments (Table 1, Tables S1) as well as others that were not differentially regulated but were predicted by algorithms (data not shown) were selected for further characterization.

To determine if putative targets were post-transcriptionally regulated by SgrS, we constructed *lacZ* translational reporter fusions under control of the P_{BAD} (arabinose-inducible) promoter (as described in Mandin and Gottesman, 2009) in hosts carrying the vector control or P_{lac}-sgrS plasmid. We tested reporter fusions to 36 candidate genes for regulation by SgrS (Fig. 1A). While the majority of the candidates showed mild (<1.5-fold) or no regulation by SgrS, translation of three genes: *asd*, *folE* and *purR* was repressed >2-fold by SgrS (Fig. 1A). Translational fusions to *gfp* confirmed post-transcriptional repression by SgrS for *asd, folE, purR* and *adiY* (Fig. 1B). Together, these results suggest that many of the changes observed in RNA-seq were due to indirect effects of SgrS on transcription and not to post-transcriptional targeting of mRNAs by SgrS. It is worth noting that many genes that were not differentially regulated in RNA-seq, but predicted computationally (data not shown), were not regulated post-transcriptionally upon ectopic production of SgrS (Fig. 1A).

Post-transcriptional regulation of asd by SgrS

To investigate SgrS regulation of *asd,* we constructed a strain where the native *asd* promoter was replaced by a constitutive Cp19 promoter (Jensen and Hammer, 1998) in wild-type and

Δ*sgrS* strains. The *asd* mRNA was detected by Northern blot in RNA samples harvested from cells at 0, 10 and 20 min. after exposure to αMG. For wild-type *E. coli*, αMG exposure resulted in reduced levels of *asd* mRNA (Fig. 2), whereas in the Δ*sgrS* background *asd* mRNA levels remained unperturbed (Fig. 2). Ectopic production of SgrS (in the absence of αMG) also promoted a reduction in *asd* mRNA levels (Fig. 2). Since transcription of *asd* in these experiments was controlled by a constitutive promoter, we conclude that SgrS promotes degradation of *asd* mRNA, consistent with *asd* being a direct target of SgrS.

To test for direct interactions between SgrS and *asd* mRNA, *in vitro* transcribed *asd* (+1 to +179 nt) and SgrS (full-length) were subjected to electrophoretic mobility shift assays (EMSAs) and footprinting. These experiments confirmed that SgrS base pairs with the 5′ region of the *asd* transcript (Figs. S2A, 3A,B,C). When unlabeled *asd* mRNA is annealed with labeled SgrS, structural changes indicated by protection and hypersensitivity are evident (Fig. 3A). The most obvious region of *asd* mRNA-dependent protection covers SgrS nts +158 to +176 (Fig. 3A). This same region is important for SgrS regulation of previously characterized targets including *ptsG* (Vanderpool and Gottesman, 2004; Rice and Vanderpool, 2011), *manX* (Rice and Vanderpool, 2011), *manY* (Rice *et al.*, 2012) and *yigL* (Papenfort et al., 2013). Interestingly, SgrS protected two different regions of *asd* mRNA (Fig. 3B, C). One region of protection overlaps the *asd* RBS (nts +32 to +49, “Site I” Fig. 3B). The second region of SgrS-dependent protection is within the *asd* coding sequence at positions +109 to +130 relative to the transcription start (“Site II” Fig. 3C). The fact that only one region of *asd*-dependent protection was observed on SgrS, suggests that same SgrS sequence can bind at two distinct sites on *asd* mRNA (Fig. 3D,E).

To elucidate the role of the two different SgrS binding sites on *asd* mRNA, we constructed translational fusions with different *asd* fragments containing both pairing sites (*asdI-II*, Fig. 4A) or each site individually (*asdI, asdII,* Fig. 4A). The results indicate that site I is absolutely required for SgrS to regulate *asd* translation. While site II is not sufficient for *asd* repression, when it is present with site I, it appears to allow tighter repression by SgrS (Fig. 4B, compare ~7.3-fold repression of *asdI-II* versus ~2.6-fold repression of *asdI*). When we introduced mutations in the *asdI* construct (*asd30-I* and *asd32-I,* Fig. 3D) that disrupt pairing at site I, the mutant fusions were no longer regulated by wild-type SgrS (Fig. 4B). Compensatory mutations in SgrS (SgrS30 and SgrS32, Fig. 3D) were defective for regulation of wild-type *asdI* (Fig. 4B), but restored regulation of the corresponding *asdI* mutant fusions (Fig. 4B). These results indicate that SgrS regulates *asd* translation by direct base pairing. In addition to translation inhibition, SgrS results in destabilization of the target transcript by recruiting RNase E. We tested whether degradation is necessary for *asd* repression by examining SgrS regulation of *asdI* and *asdI-II* constructs in wild-type and the *rne131* mutant strain deficient in degradosome assembly (Lopez *et al.*, 1999). This mutation abrogates SgrS-dependent mRNA degradation of other targets (Rice and Vanderpool, 2011; Morita *et al.*, 2004). SgrS repressed *asdI* and *asdI-II* to the same extent in wild-type and *rne131* hosts (Fig. 4B), demonstrating that RNase E is not required for SgrS-dependent translational repression of *asd* reporter fusions. To summarize, direct base pairing of SgrS at the RBS within the 5′ UTR is necessary and sufficient to inhibit translation of *asd* mRNA, however an additional SgrS binding site within the *asd* coding sequence might be important for optimal *asd* repression.

Post-transcriptional regulation of adiY *by SgrS*

In a Cp19-*adiY* strain, levels of *adiY* mRNA decreased significantly at 10 minutes and were undetectable at 15 minutes after αMG exposure in a wild-type host, but remained unchanged in the Δ*sgrS* background (Fig. 5A). When SgrS was produced ectopically in unstressed cultures, *adiY* mRNA abundance dropped rapidly (Fig. 5A). Since transcription of *adiY* in these experiments is controlled by a heterologous promoter, these results support the idea that SgrS modulates *adiY* mRNA stability.

SgrS regulates an *adiY* translational fusion containing only the *adiY* 113-nt 5′ UTR and 120 nt of coding sequence (Fig. 1B), suggesting that the SgrS binding site is within these limits. EMSAs confirmed that SgrS forms a duplex with the 5′ region of *adiY* mRNA (nts +1 to +233, Fig. S2B). Footprinting revealed that SgrS protects *adiY* mRNA in the translation initiation region, from nts +98 to +112 (Fig. 5B). The predicted SgrS-*adiY* mRNA base pairing interaction (Fig. 5C) was further tested genetically. Two mutations, *adiY1* and *adiY33* (Fig. 5C), that disrupt the interaction rendered the *adiY* reporter insensitive to wild-type SgrS (Fig. 5D). A compensatory mutation in SgrS (SgrS33) that restores pairing with *adiY33* also restored regulation (Fig. 5D). To test whether degradation of *adiY* mRNA was required for SgrS-mediated repression, *adiY* regulation was monitored in an *rne131* mutant host (Lopez *et al.*, 1999). In this host, SgrS still repressed *adiY* translation, albeit less stringently than in the *rne*$^{+}$ host (Fig. 5D). This result suggests that degradation plays a role but is not absolutely required for SgrS-mediated regulation of *adiY* mRNA. Together, these results are consistent with SgrS pairing directly at the *adiY* RBS to inhibit ribosome binding, repress translation and promote degradation of *adiY* mRNA.

Post-transcriptional regulation of folE *by SgrS*

Levels of *folE* mRNA (from Cp19-*folE*) in wild-type *E. coli* decreased after αMG addition. Under the same conditions, *folE* transcript levels remained stable in the Δ*sgrS* strain (Fig. 6A). These results are consistent with observations from RNA-seq and RT-qPCR, both showing reduced *folE* mRNA levels in SgrS-expressing cells (Table 1, Fig. S1A). SgrS binds *folE* mRNA *in vitro* (Fig. S2B). Further, translational reporter fusions *folE-long* and *folE-short* (Fig. 6B) were both regulated by SgrS, demonstrating that sequences required for SgrS-dependent regulation of *folE* reside in the 5′ UTR (Fig. 6C). IntaRNA (Busch *et al.*, 2008; Richter *et al.*, 2010) predicted that SgrS nts +158 to +174 base pair with *folE* nts +172 to +185 (Fig. 6D), which encompass the RBS and a CA-rich sequence that resembles previously described translation enhancer elements (Sharma *et al.*, 2007; Yang *et al.*, 2014). Mutations introduced into SgrS, in SgrS30 and SgrS32 (Fig. 6D) fully or partially disrupt regulation of wild-type *folE*, respectively (Fig. 6C). The compensatory mutation in *folE* (*folE32*) prevented regulation by wild-type SgrS, but restored regulation by SgrS32 (Fig. 6C). As observed for *adiY*, SgrS repressed *folE* translation more weakly in the *rne131* host, deficient in degradosome assembly (Fig. 6E). Together, these results are consistent with SgrS pairing and occluding the *folE* RBS, which leads to translation inhibition and degradation of *folE* mRNA.

Post-transcriptional regulation of purR *by SgrS*

To elucidate the region of *purR* mRNA targeted by SgrS, we made truncated *purR* mRNAs of different lengths (Fig. 7A) by *in vitro* transcription and performed EMSAs to define the region containing the SgrS binding site. Radiolabeled full-length SgrS formed higher molecular weight complexes with *purR-long* and *purR-medium*, while no shift was observed for *purR-short* (Fig. 7B). Translational reporter fusions using the same fragments, *purR-long*, *purR-medium* and *purR-short* revealed SgrS-dependent translational repression for *purR-long* and *purR-medium* but not *purR-short* (Fig. 7C). Together, these results indicated that SgrS must pair within the *purR* coding sequence between nucleotides +158 and +230 (encompassing the first 25 codons). IntaRNA predicted SgrS pairing at nts +204 to +222 of *purR* mRNA, which corresponds to codons 17-23 of *purR,* a region contained within *purR-medium*. SgrS bases +160 to +179, predicted to interact with *purR* (Fig. 7D), overlap the SgrS region that interacts with all characterized targets, including *asd, adiY* and *folE* mRNAs described in this study.

We tested regulation of *purR-medium* by SgrS30 and SgrS31, which contain mutations that disrupt the predicted base pairing (Fig. 7D). Mutants SgrS30 and SgrS31 were unable to regulate wild-type *purR-medium* (Fig. 7C). Compensatory mutations in *purR-medium* (*purR30* and *purR31*, Fig. 7D) were no longer regulated by wild-type SgrS, but regulation by SgrS30 and SgrS31, respectively, was restored (Fig. 7C). In the *rne131* background, *purR-medium* and *purR-long* were still regulated by SgrS, suggesting that RNase E-mediated degradation is not necessary for regulation (Fig. 7C). This conclusion is also supported by the finding that *purR* mRNA levels did not change when SgrS was expressed ectopically (Fig. S3, last panel). (We note that αMG affects *purR* mRNA levels in an SgrS-independent fashion (Fig. S3, first two panels).) SgrS pairs 49 to 67 nts downstream of the start codon, outside of the region occupied by the ribosome. A previous study demonstrated that sRNA binding sites within a 5-codon window could directly interfere with ribosome binding and inhibit translation (Bouvier *et al.*, 2008). Since the SgrS binding site on *purR* is well outside this window, we hypothesized that SgrS does not interfere directly with translation initiation but perhaps inhibits translation via an intermediate such as Hfq. The sRNA Spot 42, which pairs far upstream of the start codon of its target *sdhC,* was recently demonstrated to repress *sdhC* translation indirectly via recruiting Hfq to bind at a site that directly occludes ribosome binding (Desnoyers and Masse, 2012). To test whether SgrS-dependent regulation of *purR* requires Hfq, we performed *in vitro* translation. While *purR* translation was strongly repressed in the presence of both SgrS and Hfq (produced at only 7.6% of control levels, Fig. 8), SgrS alone could not efficiently block translation (57% of control levels, Fig. 8). In contrast, Hfq alone inhibited *purR* translation as well as the combination of SgrS and Hfq (8.5% of control, Fig. 8). These results are consistent with the model that Hfq itself plays the major role in inhibiting translation of *purR*, whereas SgrS alone cannot efficiently block translation. The requirement for Hfq for translational repression of *purR* contrasts with the direct SgrS-dependent repression of *ptsG* mRNA. For *ptsG,* the SgrS binding site directly overlaps the RBS (Vanderpool and Gottesman, 2004), allowing direct competition with ribosomes. Consistent with this canonical mechanism for sRNA-dependent repression, SgrS alone repressed *ptsG* translation *in vitro* almost as efficiently as the combination of SgrS plus Hfq (11.3% versus 2.8%, respectively, compared to control) whilst Hfq alone had only

a modest effect (60% of control levels, Fig. 8). The control *gfp* mRNA was translated independently of SgrS or Hfq (Fig. 8). In summary, these data are consistent with a model where SgrS base pairs within the coding sequence of *purR* mRNA and represses translation through a mechanism requiring the RNA chaperone Hfq.

Regulation of asd, adiY, folE *and* purR *by SgrS orthologs*

Orthologs of SgrS are found in numerous γ-proteobacteria such as *Salmonella*, *Erwinia amylovora*, *Klebsiella pneumoniae*, *Citrobacter koseri* and *Yersinia pestis* (Horler and Vanderpool, 2009). While the ability to regulate some targets, especially *ptsG*, appears to be widely conserved among SgrS orthologs (Horler and Vanderpool, 2009; Peer and Margalit, 2014), regulation of other targets is more variable (Rice and Vanderpool, 2011; Wadler and Vanderpool, 2009). To gain insight into whether the new targets are conserved in SgrS regulons of diverse organisms, we investigated whether SgrS orthologs could complement an *E. coli* Δ*sgrS* mutant for regulation of *E. coli* targets. SgrS orthologs from *E. amylovora*, *K. pneumoniae*, *C. koseri* and *Y. pestis* were expressed in *E. coli* reporter strains. The *asdI* reporter was not regulated by SgrS orthologs from any species other than *E. coli* (Fig. S4A), likely due to the fact that the base pairing interaction at *asd* site I is not well conserved (Fig. S4B). Predicted native SgrS-*asd* interactions from enteric species show limited and partially disrupted conservation of base pairing (Fig. S4C) suggesting that *asd* regulation by SgrS might be specifically limited to *E. coli*.

All four SgrS orthologs regulated *E. coli adiY* translation to varying degrees (Fig. S5A). The native *E. coli* SgrS-*adiY* mRNA interaction involves two stretches of complementarity (Fig. S5B). The first stretch (SgrS nucleotides +174 to +179) is highly conserved (Horler and Vanderpool, 2009; Rice and Vanderpool, 2011; Wadler and Vanderpool, 2009) while the second (nts +165 to +171) is less conserved (Fig. S5B). Although *adiY* orthologs are absent from *K. pneumoniae*, *C. koseri*, *Y. pestis and E. amylovora.* Salmonella SgrS does not show conserved complementarity with its cognate *adiY* mRNA (Fig. S5C).

For *folE*, *Y. pestis* and *C. koseri* SgrS partially repressed while *E. amylovora* and *K. pneumoniae* SgrS failed to repress translation (Fig. S6A), consistent with patterns of conservation of interacting regions (Fig. S6B). Predicted interactions of SgrS orthologs with cognate *folE* mRNAs from *Salmonella*, *K. pneumoniae*, *C. koseri*, *Y. pestis and E. amylovora* show only partial conservation of cognate base pairing interactions (Fig. S6C).

The *purR* coding sequence is highly conserved and alignment of cognate SgrS and *purR* pairs from different species shows similar predicted base pairing interactions in *E. coli*, *Salmonella*, *E. amylovora*, *K. pneumoniae* and *C. koseri* (Fig. S7). While SgrS and *purR* sequences of *Y. pestis* were very divergent, a potential region of complementarity was identified (Fig. S7). Collectively, these data suggest that SgrS regulation of *asd, adiY* and *folE* may be limited to *E. coli,* whereas *purR* is a more conserved member of the SgrS regulon.

Overexpression of new SgrS targets exacerbates glucose-phosphate stress in a ΔppsA *mutant*

Since SgrS represses each of the newly identified targets, we hypothesized that activities of the products encoded by *asd*, *adiY, folE* or *purR* are detrimental to growth under glucose-phosphate stress conditions. We tested this hypothesis by ectopic overexpression of *adiY*, *folE* and *purR* from an inducible promoter in wild-type and *sgrS* mutant strains grown under stress conditions, but did not identify any overt phenotypic differences compared to control strains (Fig. 9A, wild-type). Previous work from our laboratory implicated depletion of glycolytic intermediates as an important cause of growth inhibition of *sgrS* mutants exposed to glucose-phosphate stress conditions. Supplementation of glycolytic intermediates rescued the growth defect of an *sgrS* mutant exposed to αMG (Richards *et al.*, 2013). Overproduction of PEP synthase (encoded by *ppsA*) likewise ameliorated growth inhibition of an *sgrS* mutant during αMG-induced stress (Richards *et al.*, 2013), specifically implicating PEP as being limiting for growth under stress conditions. Therefore, we reasoned that *ppsA* mutants might be more vulnerable to depletion of PEP under stress conditions. It follows that if SgrS regulation of the newly identified targets modulates metabolism in a way that alleviates PEP depletion, we might see phenotypes associated with these targets specifically in a *ppsA* mutant background. Thus, we ectopically expressed *adiY*, *folE* and *purR* in wild-type and Δ*ppsA* strains and monitored growth on glycerol minimal plates supplemented with glucose analogs αMG or 2DG to induce glucose-phosphate stress. Ectopic expression of any of the three genes in the absence of stressors did not affect growth and was similar to uninduced controls (Fig. 9A). The Δ*ppsA* mutant carrying the vector control was more sensitive to stress caused by αMG at an early time point (Fig. 9A, 40 hr), but after 72 hours of growth, the *ppsA* mutant with vector had grown to levels similar to the wild-type strain. Notably, the *ppsA* mutant overexpressing *folE* was strongly growth inhibited compared to the *ppsA* mutant carrying the vector control when growing in the presence of either αMG or 2DG (Fig. 9A). The Δ*ppsA* mutant overexpressing *adiY* or *purR* grew similarly to the control on plates with αMG (Fig. 9A), but in the presence of 2DG, particularly at 40 hours, *adiY*- and *purR*-overexpressing cells were strongly growth inhibited compared to the control (Fig. 9A).

Similarly, we ectopically expressed *asd* in wild-type and Δ*ppsA* strains growing in minimal fructose medium supplemented with αMG to induce glucose-phosphate stress. (We used fructose as the sole carbon source because strains were sensitive to ectopically expressed *asd* when cultured in minimal glycerol medium even without induction of stress.) In the absence of stress, strains overexpressing *asd* had a slightly slower growth rate compared to vector control strains, but reached a similar final density (Fig. 9B). When cells were stressed by addition of αMG, the growth of the Δ*ppsA* mutant expressing *asd* was strongly inhibited for several hours, in contrast with other strains that all grew similarly well (Fig. 9C). To summarize, *asd*, *adiY*, *folE and purR* overexpression renders a Δ*ppsA* mutant more sensitive to glucose-phosphate stress. These observations are consistent with our hypothesis that SgrS-mediated repression of these genes modulates metabolism in a way that improves growth during stress conditions.

Discussion

Bacterial sRNAs have been shown to regulate numerous genes via short discontinuous stretches of base pairing. SgrS has served as a valuable model system to study target regulation by sRNAs in enteric bacteria such as *E. coli* and *Salmonella*. Prior to our study, *E. coli* SgrS was known to directly regulate three mRNAs: *ptsG*, *manXYZ* and *yigL* (Papenfort *et al.*, 2013; Rice and Vanderpool, 2011; Vanderpool and Gottesman, 2004). In addition to these targets, in *Salmonella,* SgrS negatively regulates the *Salmonella*-specific *sopD* mRNA, encoding a secreted virulence effector protein (Papenfort *et al.*, 2012). Here, we substantially expand the SgrS regulon by defining *asd*, *adiY*, *folE* and *purR* as direct targets of *E. coli* SgrS (Figs. 2-8).

In this study, we show that pulse expression of SgrS (in the absence of stress) yields a narrow spectrum of changes in gene expression. In addition to affecting known targets (*ptsG, manXYZ* and *yigL*) and newly identified targets (*asd*, *adiY*, *folE* and *purR*), SgrS pulse expression also altered levels of mRNAs encoding functions involved in metal homeostasis (zinc-related genes *zinT* and *znuABC* and copper homeostasis genes *cusF* and *cusC*), predicted transporters (*nepI, ydjN*) and poorly characterized genes (*yeeD, pliG, yeiB, yebA, ykgM*) (Table 1). Though RT-qPCR confirmed the SgrS-dependent changes in mRNA levels for the majority of these genes, further analysis indicated that the effects were not post-transcriptional (Fig. 1A), suggesting that these mRNAs are not direct targets of SgrS. To facilitate efforts to better predict direct SgrS targets in future searches, we elucidated an SgrS-recognition motif based on the known SgrS base pairing sites. The multiple Em for motif elicitation tool (MEME) (Bailey and Gribskov, 1998) was used to align *ptsG, manX, manY, yigL, asd* (sites I and II), *adiY, folE* and *purR* SgrS binding sites (Fig. S8A). The consensus SgrS binding site based on these targets is G/C-rich and contains a prominent 5′-ACRCA-3′ motif (Fig. S8B), which is complementary with two sites on SgrS. The first SgrS site comprises a 5′-UGAGU-3′ sequence at positions +175 to +179, and includes two nucleotides (G176 and G178) shown to be crucial for regulation of *ptsG* mRNA (Kawamoto *et al.*, 2006; Wadler and Vanderpool, 2007). The second SgrS site contains the 5′-UGUGU-3′ sequence responsible for interaction with *manX* mRNA, where G168 and G170 are crucial for regulation of this target (Rice and Vanderpool, 2011). Identifying the 5′-ACRCA-3′ motif in other mRNAs that are differentially expressed in response to SgrS production might improve prediction of additional members of the SgrS regulon.

Our analyses of the new SgrS targets revealed diversity in the mechanisms SgrS employs to post-transcriptionally regulate *asd*, *adiY*, *folE* and *purR*. In the common mode of sRNA-mediated repression, SgrS base pairs within the 5′ UTR of *asd*, *adiY and folE,* occluding the RBS, which interferes with translation initiation. Optimal repression of *asd,* however, involves an additional SgrS interaction with a binding site in the coding sequence of *asd*. We note that SgrS pairs at two distinct sites on another target, *manXYZ* mRNA, and that pairing at both sites is required to promote degradation of *manXYZ* mRNA and increase the stringency of regulation (Rice *et al.*, 2012). It remains possible that the two SgrS binding sites on *asd* play a similar role in promoting *asd* mRNA degradation, or that another step of regulation is affected by the involvement of two binding sites. In both cases, *manXYZ* and

asd, further work will be required to elucidate the molecular mechanism of SgrS-mediated regulation via binding at two sites.

The SgrS binding site within the *purR* coding sequence is too far downstream of the translation initiation region to directly occlude ribosome binding. Instead, we hypothesize that SgrS indirectly represses translation of *purR* by a 'role reversal' with Hfq, similar to the mechanism defined for Spot 42-dependent regulation of *sdhC* mRNA (Desnoyers and Masse, 2012). Spot 42 pairs upstream of the *sdhC* RBS and cannot directly interfere with the ribosome binding, while recruiting Hfq effectively blocks translation initiation. Unlike canonical mechanisms where the sRNA directly inhibits translation, it can also play a chaperone role of providing target specificity for Hfq (Desnoyers and Masse, 2012). Our *in vitro* translation analyses show that SgrS is sufficient for repression of a target known to be regulated by direct ribosome occlusion (Fig. 8, PtsG-FLAG), whereas for *purR,* Hfq alone can repress translation while SgrS alone has a very modest effect (Fig. 8, PurR-FLAG). Our data are consistent with a model where SgrS, *purR* mRNA and Hfq form a nucleoprotein complex, and that SgrS promotes binding of Hfq in the translation initiation region where it can directly interfere with ribosome binding. Combined with published work (Vanderpool and Gottesman, 2004; Rice and Vanderpool, 2011; Rice *et al.*, 2012; Papenfort *et al.*, 2013; Papenfort *et al.*, 2012; Kawamoto *et al.*, 2006), our results add to the already impressive variety of mechanisms SgrS employs to regulate target genes.

While it is clear that SgrS represses translation of each of the newly identified targets by a base pairing-dependent mechanism, the underlying physiological role for this repression is not precisely clear. The four new targets encode enzymes (*asd*, *folE*) or regulators (*adiY, purR*) of diverse metabolic pathways. We show that aberrant overexpression of each of them yields stress-dependent growth defects of varying severity, specifically in a host compromised for PEP synthesis from pyruvate (*ppsA* mutant, Fig. 9). Since our previous work implicates depletion of glycolytic intermediates (particularly PEP) as an important cause of growth inhibition during stress (Richards *et al.*, 2013), we posit that SgrS-mediated regulation of these new targets modifies metabolism to promote replenishment of one or more limiting metabolites, possibly PEP or other glycolytic intermediates that can be synthesized from PEP.

One way to replenish the pool of PEP is through PpsA that uses pyruvate as a substrate (Fig. 10). Mutants lacking *ppsA* are indeed more susceptible to growth inhibition due to accumulation of non-metabolizable glucose analogs (Kornberg and Lambourne, 1994). Alternative to the PpsA pathway, PEP carboxykinase (Pck) can produce PEP from oxaloacetate (OAA), a TCA cycle intermediate (Fig. 10). Aspartate can be converted to OAA by the enzyme aspartate transaminase (AspC), linking aspartate metabolism to glycolysis (Fig. 10). Moreover, supplementing aspartate in the growth medium can partially relieve the glucose-phosphate stress-related growth defect of a *ppsA* mutant strain (Kornberg and Lambourne, 1994). Previous analysis of carbon metabolism in *E. coli* indicates that OAA to PEP conversion is important in the strain defective in PTS-mediated sugar transport. Specifically, carbon flux through Pck was shown to respond to changes in PEP availability in the cell (Flores *et al.*, 2002). Pck was also suggested to stimulate glycolytic flux under the conditions of reduced carbon flux due to defects in PTS (Meza *et al.*, 2012). We hypothesize

that SgrS regulation of *asd* expression might increase the pool of available aspartate that can be converted by AspC to OAA, which is then used by Pck to replenish PEP (Fig. 10). Accordingly, our results demonstrate that ectopic expression of *asd* in glucose-phosphate stress-sensitive strain (Δ*ppsA* mutant strain) is growth inhibitory (Fig. 9B, C).

The *adiY* gene encodes a regulator that activates transcription of *adiA*, encoding an arginine decarboxylase involved in arginine-dependent acid resistance. AdiA converts arginine to agmatine and in the process consumes intracellular protons, which helps to raise cytosolic pH. Agmatine is then exchanged for an additional arginine from the environment by a symporter AdiC (Castanie-Cornet *et al.*, 1999). Interestingly, AdiY is only active under anaerobic conditions (Stim-Herndon *et al.*, 1996). The arginine decarboxylase used for biosynthesis under aerobic conditions is encoded by *speA,* and we note that SgrS had no effect on *speA* mRNA levels in pulse expression experiments (Table 1). This suggests that perhaps the role of SgrS in modulating the arginine decarboxylase pathway (through *adiY* regulation and indirect effects on *adiA*) may not be physiologically relevant under our particular (aerobic) stress conditions. We have not explored the nature of glucose-phosphate stress or SgrS-dependent phenotypes under anaerobic conditions, thus we cannot speculate further on a possible rationale for SgrS-mediated regulation of *adiY* under these conditions.

On the whole, members of the SgrS target regulon are functionally quite diverse. Our previous studies clearly demonstrate that the physiological importance of regulation of particular SgrS targets is variable and depends on the specific growth conditions. Regulation of *ptsG* alone is sufficient to rescue growth in the presence of αMG when cells are growing in rich medium (LB), but in minimal media, stress results in more pronounced growth inhibition that cannot be rescued by regulation of *ptsG* alone. Instead, when cells are growing in nutrient-poor minimal media and stressed by exposure to αMG, SgrS-mediated repression of *ptsG* and activation of *yigL* is necessary, but not sufficient for full growth rescue (Sun and Vanderpool, 2013). In contrast, regulation of *ptsG* and *yigL* is dispensable when cells are stressed by another glucose analog, 2DG (2-deoxy glucose). SgrS-mediated regulation of *manXYZ* is required for growth rescue in the presence of 2DG (Rice and Vanderpool, 2011). We postulate that SgrS-mediated regulation of newly characterized targets *asd*, *adiY*, *folE* and *purR* may be required only under specific conditions that we have not yet defined. Based on the observation that overexpression of these targets is detrimental specifically in stressed cells in a host background with compromised PEP metabolism, we predict that modulation of these targets by SgrS will be most important under stress conditions that put a severe strain on metabolic flux. Regulation of *asd*, *adiY*, *folE* and *purR* under such conditions could help restore metabolic homeostasis.

Although SgrS is conserved among enteric bacteria, the diversity of its target regulon is evident. In *Salmonella,* in addition to *ptsG*, *manXYZ* and *yigL*, the *sopD* mRNA is repressed by SgrS (Papenfort *et al.*, 2012). The *sopD* gene is encoded on a *Salmonella* pathogenicity island, so this target is only part of the *Salmonella* SgrS regulon. Species-specific regulation by SgrS is also highlighted by the finding that *Erwinia* and *Yersinia* SgrS orthologs do not regulate their cognate *manXYZ* orthologs (Rice and Vanderpool, 2011). Current evidence suggests that SgrS and other base pairing-dependent sRNA regulators evolved as a result of establishing a regulatory interaction with one primary target mRNA,

while additional targets in the regulon adopted sequences complementary to the sRNA allowing their regulation (Peer and Margalit, 2014). Considering SgrS conservation and distribution among γ-proteobacteria suggest a fairly ancient origin of this sRNA (Horler and Vanderpool, 2009; Skippington and Ragan, 2012), it is conceivable that different sets of genes in different organisms, sometimes including horizontally acquired genes like *Salmonella sopD* (Papenfort et al., 2012), evolved binding sites and established regulatory relationships with SgrS. The present study shows that *E. coli* SgrS regulates *adiY,* which is not conserved among other enteric species (Fig. S5C), and thus represents an *E. coli*-specific target of SgrS. Regulation of *asd*, *folE* and *purR* also appears to be narrowly distributed phylogenetically, as SgrS orthologs have only partially conserved base pairing interactions with their cognate *asd*, *folE* and *purR* mRNAs (Figs. S4C, S6C, S7). Full elucidation of SgrS regulons in diverse organisms will help us understand how target regulons evolve along with their sRNA regulator, and shed light on roles played by SgrS in helping enteric bacteria cope with stresses that they experience in their specific environmental niches.

It is evident that glucose-phosphate stress alters cellular metabolic balance, which results in a plethora of changes in the gene expression. Glycolysis is a central metabolic pathway that provides intermediates for biosynthesis of numerous cellular macromolecules and also generates energy by substrate-level phosphorylation. Imbalanced glycolytic metabolism thus has potentially very broad impacts not only locally, but also systemically. Our previous work demonstrates that SgrS plays a central role in recovery from glucose-phosphate stress by reducing uptake of non-metabolizable sugars through repression of genes encoding sugar transporters (Rice and Vanderpool, 2011; Vanderpool and Gottesman, 2004) and enhancing efflux of sugars via activating a phosphatase whose activity is a prerequisite for efflux of sugars (Papenfort *et al.*, 2013). Our current work demonstrates that the effects of SgrS extend beyond regulation of sugar uptake and efflux and imply that SgrS regulation of diverse metabolic pathways may contribute to the stress response under some circumstances. We hypothesize that SgrS-dependent regulation of the newly described targets *asd*, *adiY*, *folE* and *purR* mRNAs helps restore metabolic homeostasis in order to promote recovery from glucose-phosphate stress.

Experimental Procedures

Strain and plasmid construction

Strains and plasmids used in this study are listed in Table S2. All strains used in this study are derivatives of *E. coli* K-12 strain MG1655. Oligonucleotide primers and 5′-biotinylated probes used in this study are listed in Table S3 and were acquired from Integrated DNA Technologies. Chromosomal mutations were made by λ Red recombination (Yu *et al.*, 2000; Datsenko and Wanner, 2000) and marked alleles were moved between strains by P1 *vir* transduction (Miller, 1972).

Alleles kan^R::Cp19-*asd,* kan^R::Cp19-*adiY,* kan^R::Cp19-*folE* and kan^R::Cp19-*purR* were constructed by PCR amplifying kan^R-linked Cp19 constitutive promoter from JNB024 chromosomal DNA using oligonucleotides MBP23F/MBP23R, MBP24F/MBP24R, MBP25F/MBP25R, MBP181F/MBP181R containing *asd*, *adiY, folE* or *purR* homologies, respectively (previously described in (Rice and Vanderpool, 2011). PCR products were

recombined into NM200 strain. The resulting alleles were moved by transduction into wild-type (DJ480) and Δ*sgrS* (JH111), or rne131 (JH256) backgrounds to generate desired strains (Table S2).

FLAG-tagged alleles were constructed by amplifying 3×FLAG::FRT-kan^R-FRT cassette from pSUB11 using primers MBP204F2/MBP204R2 and MBP211F/ MBP211R containing overhangs homologous to *purR* and *ptsG*, respectively. PCR products were recombined into NM200 strain to produce MB138 and MB158 strains.

Translational *lacZ* reporter fusions under the control of the P_{BAD} promoter were constructed by PCR amplifying fragment of interest using primers containing 5′ homologies to P_{BAD} and *lacZ* (Table S3). PCR products were recombined into PM1205 using λ Red homologous recombination and counter-selection against *sacB* as described previously (Mandin and Gottesman, 2009).

Plasmids harboring *sgrS* orthologs under the control of the $P_{LtetO-1}$ promoter were constructed by PCR amplifying *sgrS* from *E. coli* MG1655, *Yersinia pestis*, *Klebsiella pneumoniae*, *Erwinia carotovora* and *Citrobacter koseri* chromosomal DNA using oligonucleotides containing NdeI and BamHI restriction sites (Table S3). PCR products and vector pZA31R (Levine *et al.*, 2007) were digested with NdeI and BamHI (New England Biolabs) restriction endonucleases. Digestion products were ligated using DNA Ligase (New England Biolabs) to produce plasmids containing $P_{LtetO-1}$-*sgrS* alleles (Table S2).

Plasmid pZEMB8 containing $P_{LlacO-1}$-*ptsG-gfp* was constructed by PCR amplifying *ptsG* from MG1655 chromosomal DNA using oligos MBP1L and MBP1R10 containing EcoRI and KpnI restriction sites, respectively. The PCR product and vector pZE12S (Levine *et al.*, 2007) were digested with KpnI and EcoRI restriction endonucleases. Digestion products were ligated using DNA Ligase to produce pZEMB2. Superfolder *gfp* (*gfpsf*) was amplified from pXG10-SF (Corcoran *et al.*, 2012) using oligonucleotides gfpsf-F and gfpsf-R, respectively containing KpnI and XbaI restriction sites. pZEMB2 and the resulting PCR product were digested with KpnI and XbaI, and ligated with DNA Ligase to produce pZEMB8. Oligonucleotides MBP92F/MBP92R1, MBP29F2/MBP29R40 and MBP30F/ MBP30R40 were used to PCR amplify *asd*, *adiY* and *folE*, respectively. Fragments of *asd, adiY* and *folE* were digested with KpnI and EcoRI and cloned into pZEMB8 to obtain desired translational *gfp* reporter fusions (Table S2). Plasmids containing mutant alleles of *adiY* were generated by QuikChange mutagenesis procedure using oligonucleotides with mismatched bases at desired locations (Table S3).

Overexpression plasmids containing full-length *asd*, *adiY*, *folE* and *purR* genes under the control of the P_{lac} promoter were constructed by PCR amplifying genes of interest using (respectively) oligonucleotides MBP138F/MBP138R, MBP152F/MBP152R, MBP153F/ MBP153R and MBP154F/MBP154R, and restriction cloning into pBRCS12 using BamHI and HindIII restriction endonucleases.

Media and reagents

Bacteria were cultured in Luria-Bertani (LB) broth medium or on LB agar plates at 37°C, unless stated otherwise. Bacteria were grown in MOPS (morpholine-propanesulfonic acid) rich defined medium (Teknova) with 0.2% fructose for reporter fluorescence assays and LB medium for Northern blot experiments. M63 minimal medium supplemented with 0.4% glycerol was used for plate assays and M63 minimal medium with 0.2% fructose was used for growth curves. Where necessary, media were supplemented with antibiotics at following concentrations: 100 μg ml^{-1} ampicillin (Amp), 25 μg ml^{-1} chloramphenicol (Cm), 25 μg ml^{-1} kanamycin (Kan). Isopropyl β-D-1-thiogalactopyranoside (IPTG) was used at concentrations of 0.5 mM or 1 mM for induction of expression from $P_{LlacO-1}$ promoter and anhydrotetracycline (aTc) at 30 ng ml^{-1} for induction of $P_{Ltet0-1}$ promoter. Glucose-phosphate stress was induced where appropriate using 0.5% αMG or 60 μM 2DG, unless stated otherwise.

RNA-seq analysis

E. coli strain CV104 (Δ*sgrS*) harboring vector (pHDB3) or P_{lac}-*sgrS* (pLCV1) plasmid was grown to OD_{600}~0.5 in MOPS rich medium supplemented with 0.2% D-glucose and exposed to 0.1 mM IPTG for 10 minutes. Previously described hot phenol method (Aiba *et al.*, 1981) was used to extract total RNA, which was treated with TURBO™ DNase (Ambion) according to manufacturer's protocol and resolved by electrophoresis on 1.2 % agarose gel to confirm integrity. Ribosomal RNA removal, library construction and sequencing were performed at the W. M. Keck Center for Comparative and Functional Genomics at the University of Illinois at Urbana-Champaign. Ribosomal RNA was removed from 1 μg of total RNA using Ribozero rRNA Removal Meta-Bacteria Kit (Epicentre Biotechnologies) and the mRNA-enriched fraction was converted to indexed RNA-seq libraries with the ScriptSeq™ v2 RNA-Seq Library Preparation Kit (Epicentre Biotechnologies). The libraries were pooled in equimolar concentrations and were quantitated by qPCR with the Library Quantification kit Illumina compatible (Kapa Biosystems) and sequenced for 101 cycles plus 7 cycles for the index read on a HiSeq2000 using TruSeq SBS version 3 reagents. The output fastq files were generated using Casava 1.8.2 (Illumina) and analyzed with Rockhopper (McClure *et al.*, 2013) for computational analysis of bacterial RNA-seq data.

Reporter fluorescence assay

Bacterial strains were cultured overnight in MOPS rich medium supplemented with 0.2% fructose, Amp, Cm and subcultured 1:100 to fresh medium with appropriate inducers (IPTG, aTc) in 48 well plates. Relative fluorescence units (RFU) and optical density (OD_{600}) were measured during mid-exponential phase of growth. RFU normalized to OD_{600} was calculated and plotted relative to IPTG only control (RFU/OD_{600}).

β-galactosidase assay

Bacterial strains were cultured overnight in Terrific Broth (TB) with Amp and subcultured 1:100 to fresh TB medium containing Amp and 0.002% L-arabinose. Cells were grown at 37°C with shaking to OD_{600}~0.15 and 0.1 mM IPTG was added to induce expression from

the plasmid and cells grown for another hour to OD_{600}~0.5-0.6. β-galactosidase assays were then performed according to previously described protocol (Miller, 1972).

Quantitative real time polymerase chain reaction (RT-qPCR)

E. coli strain CV104 (Δ*sgrS*) harboring vector (pHDB3) or P_{lac}-*sgrS* (pLCV1) plasmids were cultured in MOPS rich medium with 0.2% D-glucose to OD_{600}~0.5 and total RNA extracted (Aiba *et al.*, 1981) at 10 minutes after addition of 0.1 mM IPTG. As an exception, total RNA for detection of *adiY* expression was extracted from still cultures, due to higher *adiY* expression in partially anaerobic conditions. cDNA was generated from 2 μg of RNA in a reverse transcriptase PCR reaction primed with Random Hexamers (Roche). Sample preparation was performed according to Power SYBR Green PCR Master Mix (Applied Biosystems) specifications and qPCR was used to analyze relative expression levels using gene-specific primers (Table S3). Software supplemented with Mastercycler ep realplex (Eppendorf) thermocycler was used for relative quantification of expression. The relative mRNA levels were normalized to a housekeeping gene *rrsA* encoding 16S rRNA in *E. coli*.

Northern blot analysis

Bacterial strains were cultured in LB medium to OD_{600}~0.4. Total RNA was extracted as described previously (Aiba *et al.*, 1981) at specified times after addition of 0.5% αMG to induce stress or 0.1 mM IPTG to induce expression of SgrS from the plasmid. RNA concentrations were measured spectrophotometrically and 15 μg of RNA were resolved using 1.2 % agarose gel electrophoresis at 90 V for 1.5 h. For detection of SgrS, 10 μg of RNA were resolved on 8% polyacrylamide urea gel by running at 100V for 1 h. RNA was transferred to 0.2 μm pore-size Nytran N (Whatman) membrane as described previously (Majdalani *et al.*, 2001). Membrane was prehybridized for 45 min in ULTRAhyb (Ambion) solution at 42°C. Blots were hybridized overnight with 5′-biotinylated ryaA1-bio, MBP-asd-bio, MBP-adiY-bio, MBP-folE-bio, MBP-purR-bio2 or ssrA-bio probes specific for SgrS, *asd*, *adiY*, *folE*, *purR* and *ssrA* respectively (Table S3). BrightStar BioDetect kit (Ambion) was used for detection.

In vitro *transcription*

Template DNA for *in vitro* transcription was generated by PCR using gene-specific oligonucleotides containing the T7 promoter sequence. Following oligonucleotides were used to generate specific template DNA: MBP56F/MBP56R–*asd* (+1 to +179), MBP57F/MBP57R–*adiY* (+1 to +233), MBP94F/MBP94R–*folE* (+112 to +300), MBP65F/MBP65R–*purR-long* (+1 to +299), MBP65F/MBP174R–*purR-medium* (+1 to +230), MBP65F/MBP178R–*purR-short* (+1 to +158), MBP65F/MBP205R2–*purR*-3×FLAG, MBP84F/MBP205R2–*ptsG*-3×FLAG, O-SA070/ O-SA071–*gfp* and O-JH219/O-JH119 were used to generate full-length *sgrS* template DNA. *In vitro* transcription of DNA templates was performed according to specifications of MEGAscript T7 Kit (Ambion).

In vitro *translation and Western blot analysis*

In vitro transcribed RNA was denatured by mixing 1 pmol of *purR* or *ptsG* with 10 pmol of SgrS and 0.5 pmol of *gfp* (control), and incubated at 65°C for 5 min. Samples were placed

on ice for 5 minutes and 4 Units of SUPERase-In (Ambion) and 10 pmol of Hfq were added to the reactions. RNA was preincubated with 3.5 μl of 2x binding buffer (20 mM Tris·HCl, pH 8.0; 1 mM DTT; 1 mM MgCl2; 20 mM KCl; and 10 mM Na2HPO4–NaH2PO4, pH 8.0) for 30 min at 37°C (modified from (Maki *et al.*, 2008) and translation was performed using PURExpress *In Vitro* Protein Synthesis Kit (New England Biolabs), according to manufacturer's protocol. Translation reactions were terminated by adding Laemmli sample buffer (Bio-Rad) and heated to 95°C for 10 min. Synthesized proteins were resolved for 45 min at 150 V on NuPAGE 4-12% Bis-Tris Gel (Life Technologies) and transferred to Immobilon-P^{SQ} membrane (Millipore). The membranes were treated with monoclonal anti-FLAG M2 antibody (Sigma-Aldrich) or polyclonal anti-GFP antibody (Thermo Scientific). Signals were visualized by Pierce ECL Western blotting substrate (Thermo Scientific). Band densities were measured using ImageJ (http://imagej.nih.gov/ij/).

RNA-RNA gel electromobility shift assay

In vitro transcribed RNA was 5′-end labeled with radioisotope ^{32}P using the KinaseMax Kit (Ambion). Subsequently, 20 or 100 pmol of unlabeled SgrS, *asd*, *adiY* or *folE* RNA were mixed with 0.1 pmol of 5′-end labeled SgrS or *asd* RNA. Similarly, 0.2, 2 or 20 pmol of unlabeled *purR* RNA were hybridized with 0.2 pmol of 5′-end labeled SgrS RNA. Samples were denatured at 95°C for 1 min, re-natured on ice for 5 min, and hybridized at 37°C for 30 min in 1x Structure Buffer (Ambion). Non-denaturing loading buffer was added and samples resolved for 6 h at 40 V on native 5.6% PAGE.

RNA-RNA footprinting analysis

In vitro transcribed RNA was 5′-end labeled with radioisotope ^{32}P using the KinaseMax Kit (Ambion). Footprinting reactions were performed according to previously published protocol (Desnoyers *et al.*, 2009) with the following modifications: 20 pmol of unlabeled SgrS or *asd* RNA were incubated with 0.1 pmol of 5'-end labeled *asd* or SgrS RNA respectively, at 37°C for 30 min in 1x Structure Buffer (Ambion) in the presence or absence of 300nM Hfq. Also, 20 pmol and 100 pmol of unlabeled SgrS RNA were incubated at 37°C for 30 min in 1x Structure Buffer (Ambion) with 0.1 pmol of 5'-end labeled *adiY* RNA.

Supplementary Material

Refer to Web version on PubMed Central for supplementary material.

Acknowledgements

We would like to extend a special thank you to Brian Tjaden for his invaluable help with RNA-seq data analysis. We are grateful to Jennifer Rice, Rich Yemm, Divya Balasubramanian, Chelsea Lloyd, Yan Sun, Gregory Richards, Richard Horler, Shafiul Azam, Alisa King, Jessica Kelliher and other current and past members of the Vanderpool lab for strains, plasmids, stimulating discussions and valuable advise. We appreciate and extend our thank you to James Slauch and members of his lab for fruitful discussions. This work was supported by the National Institutes of Health (grant R01 GM092830), and a University of Illinois Department of Microbiology James R. Beck Fellowship (to M. B.).

References

Aiba H, Adhya S, de Crombrugghe B. Evidence for two functional *gal* promoters in intact *Escherichia coli* cells. J. Biol. Chem. 1981; 256:11905–11910. [PubMed: 6271763]

Altuvia S, Weinstein-Fischer D, Zhang A, Postow L, Storz G. A small, stable RNA induced by oxidative stress: role as a pleiotropic regulator and antimutator. Cell. 1997; 90:43–53. [PubMed: 9230301]

Bailey TL, Gribskov M. Combining evidence using p-values: application to sequence homology searches. Bioinformatics. 1998; 14:48–54. [PubMed: 9520501]

Barupal DK, Lee SJ, Karoly ED, Adhya S. Inactivation of metabolic genes causes short- and long-range dys-regulation in Escherichia coli metabolic network. PLoS One. 2013; 8:e78360. [PubMed: 24363806]

Bobrovskyy M, Vanderpool CK. Regulation of bacterial metabolism by small RNAs using diverse mechanisms. Annual review of genetics. 2013; 47:209–232.

Bouvier M, Sharma CM, Mika F, Nierhaus KH, Vogel J. Small RNA binding to 5′ mRNA coding region inhibits translational initiation. Mol Cell. 2008; 32:827–837. [PubMed: 19111662]

Busch A, Richter AS, Backofen R. IntaRNA: efficient prediction of bacterial sRNA targets incorporating target site accessibility and seed regions. Bioinformatics. 2008; 24:2849–2856. [PubMed: 18940824]

Castanie-Cornet MP, Penfound TA, Smith D, Elliott JF, Foster JW. Control of acid resistance in Escherichia coli. J Bacteriol. 1999; 181:3525–3535. [PubMed: 10348866]

Corcoran CP, Podkaminski D, Papenfort K, Urban JH, Hinton JC, Vogel J. Superfolder GFP reporters validate diverse new mRNA targets of the classic porin regulator, MicF RNA. Mol Microbiol. 2012; 84:428–445. [PubMed: 22458297]

Datsenko KA, Wanner BL. One-step inactivation of chromosomal genes in *Escherichia coli* K-12 using PCR products. Proc. Natl. Acad. Sci. USA. 2000; 97:6640–6645. [PubMed: 10829079]

Desnoyers G, Masse E. Noncanonical repression of translation initiation through small RNA recruitment of the RNA chaperone Hfq. Genes Dev. 2012; 26:726–739. [PubMed: 22474262]

Desnoyers G, Morissette A, Prévost K, Massé E. Small RNA-induced differential degradation of the polycistronic mRNA iscRSUA. EMBO J. 2009; 28:1551–1561. [PubMed: 19407815]

Englesberg E, Anderson RL, Weinberg R, Lee N, Hoffee P, Huttenhauer G, Boyer H. L-Arabinose-sensitive, L-ribulose 5-phosphate 4-epimerase-deficient mutants of Escherichia coli. Journal of bacteriology. 1962; 84:137–146. [PubMed: 13890280]

Flores S, Gosset G, Flores N, de Graaf AA, Bolivar F. Analysis of carbon metabolism in Escherichia coli strains with an inactive phosphotransferase system by (13)C labeling and NMR spectroscopy. Metab Eng. 2002; 4:124–137. [PubMed: 12009792]

Frohlich KS, Papenfort K, Fekete A, Vogel J. A small RNA activates CFA synthase by isoform-specific mRNA stabilization. EMBO J. 2013; 32:2963–2979. [PubMed: 24141880]

Horler RS, Vanderpool CK. Homologs of the small RNA SgrS are broadly distributed in enteric bacteria but have diverged in size and sequence. Nucleic Acids Res. 2009; 37:5465–5476. [PubMed: 19531735]

Irani MH, Maitra PK. Properties of Escherichia coli mutants deficient in enzymes of glycolysis. Journal of bacteriology. 1977; 132:398–410. [PubMed: 410789]

Jensen PR, Hammer K. The sequence of spacers between the consensus sequences modulates the strength of prokaryotic promoters. Appl Environ Microbiol. 1998; 64:82–87. [PubMed: 9435063]

Kawamoto H, Koide Y, Morita T, Aiba H. Base-pairing requirement for RNA silencing by a bacterial small RNA and acceleration of duplex formation by Hfq. Mol Microbiol. 2006; 61:1013–1022. [PubMed: 16859494]

Kimata K, Tanaka Y, Inada T, Aiba H. Expression of the glucose transporter gene, ptsG, is regulated at the mRNA degradation step in response to glycolytic flux in Escherichia coli. EMBO J. 2001; 20:3587–3595. [PubMed: 11432845]

Kornberg H, Lambourne LT. The role of phosphoenolpyruvate in the simultaneous uptake of fructose and 2-deoxyglucose by Escherichia coli. Proceedings of the National Academy of Sciences of the United States of America. 1994; 91:11080–11083. [PubMed: 7972013]

Kruger J, Rehmsmeier M. RNAhybrid: microRNA target prediction easy, fast and flexible. Nucleic Acids Res. 2006; 34:W451–454. [PubMed: 16845047]

Lease RA, Cusick ME, Belfort M. Riboregulation in Escherichia coli: DsrA RNA acts by RNA:RNA interactions at multiple loci. Proceedings of the National Academy of Sciences of the United States of America. 1998; 95:12456–12461. [PubMed: 9770507]

Lee SJ, Trostel A, Adhya S. Metabolite changes signal genetic regulatory mechanisms for robust cell behavior. mBio. 2014; 5:e00972–00913. [PubMed: 24473130]

Lee SJ, Trostel A, Le P, Harinarayanan R, Fitzgerald PC, Adhya S. Cellular stress created by intermediary metabolite imbalances. Proc Natl Acad Sci U S A. 2009; 106:19515–19520. [PubMed: 19887636]

Levine E, Zhang Z, Kuhlman T, Hwa T. Quantitative characteristics of gene regulation by small RNA. PLoS Biol. 2007; 5:e229. [PubMed: 17713988]

Lopez PJ, Marchand I, Joyce SA, Dreyfus M. The C-terminal half of RNase E, which organizes the Escherichia coli degradosome, participates in mRNA degradation but not rRNA processing in vivo. Mol Microbiol. 1999; 33:188–199. [PubMed: 10411735]

Majdalani N, Chen S, Murrow J, St John K, Gottesman S. Regulation of RpoS by a novel small RNA: the characterization of RprA. Mol Microbiol. 2001; 39:1382–1394. [PubMed: 11251852]

Maki K, Uno K, Morita T, Aiba H. RNA, but not protein partners, is directly responsible for translational silencing by a bacterial Hfq-binding small RNA. Proc Natl Acad Sci U S A. 2008; 105:10332–10337. [PubMed: 18650387]

Mandin P, Gottesman S. A genetic approach for finding small RNAs regulators of genes of interest identifies RybC as regulating the DpiA/DpiB two-component system. Mol Microbiol. 2009; 72:551–565. [PubMed: 19426207]

Masse E, Escorcia FE, Gottesman S. Coupled degradation of a small regulatory RNA and its mRNA targets in Escherichia coli. Genes & development. 2003; 17:2374–2383. [PubMed: 12975324]

Masse E, Gottesman S. A small RNA regulates the expression of genes involved in iron metabolism in Escherichia coli. Proceedings of the National Academy of Sciences of the United States of America. 2002; 99:4620–4625. [PubMed: 11917098]

Masse E, Salvail H, Desnoyers G, Arguin M. Small RNAs controlling iron metabolism. Current opinion in microbiology. 2007; 10:140–145. [PubMed: 17383226]

McClure R, Balasubramanian D, Sun Y, Bobrovskyy M, Sumby P, Genco CA, Vanderpool CK, Tjaden B. Computational analysis of bacterial RNA-Seq data. Nucleic Acids Res. 2013; 41:e140. [PubMed: 23716638]

Meza E, Becker J, Bolivar F, Gosset G, Wittmann C. Consequences of phosphoenolpyruvate:sugar phosphotranferase system and pyruvate kinase isozymes inactivation in central carbon metabolism flux distribution in Escherichia coli. Microb Cell Fact. 2012; 11:127. [PubMed: 22973998]

Miller, JH. Experiments in molecular genetics. Cold Spring Harbor Laboratory; Cold Spring Harbor, New York: 1972. p. 466

Moller T, Franch T, Hojrup P, Keene DR, Bachinger HP, Brennan RG, Valentin-Hansen P. Hfq: a bacterial Sm-like protein that mediates RNA-RNA interaction. Molecular cell. 2002; 9:23–30. [PubMed: 11804583]

Morfeldt E, Taylor D, von Gabain A, Arvidson S. Activation of alpha-toxin translation in Staphylococcus aureus by the trans-encoded antisense RNA, RNAIII. The EMBO journal. 1995; 14:4569–4577. [PubMed: 7556100]

Morita T, El-Kazzaz W, Tanaka Y, Inada T, Aiba H. Accumulation of glucose 6-phosphate or fructose 6-phosphate is responsible for destabilization of glucose transporter mRNA in Escherichia coli. The Journal of biological chemistry. 2003; 278:15608–15614. [PubMed: 12578824]

Morita T, Kawamoto H, Mizota T, Inada T, Aiba H. Enolase in the RNA degradosome plays a crucial role in the rapid decay of glucose transporter mRNA in the response to phosphosugar stress in *Escherichia coli*. Mol Microbiol. 2004; 54:1063–1075. [PubMed: 15522087]

Morita T, Maki K, Aiba H. RNase E-based ribonucleoprotein complexes: mechanical basis of mRNA destabilization mediated by bacterial noncoding RNAs. Genes & development. 2005; 19:2176–2186. [PubMed: 16166379]

Obana N, Shirahama Y, Abe K, Nakamura K. Stabilization of Clostridium perfringens collagenase mRNA by VR-RNA-dependent cleavage in 5′ leader sequence. Molecular microbiology. 2010; 77:1416–1428. [PubMed: 20572941]

Opdyke JA, Kang JG, Storz G. GadY, a small-RNA regulator of acid response genes in Escherichia coli. J Bacteriol. 2004; 186:6698–6705. [PubMed: 15466020]

Papenfort K, Podkaminski D, Hinton JC, Vogel J. The ancestral SgrS RNA discriminates horizontally acquired Salmonella mRNAs through a single G-U wobble pair. Proceedings of the National Academy of Sciences of the United States of America. 2012; 109:E757–764. [PubMed: 22383560]

Papenfort K, Sun Y, Miyakoshi M, Vanderpool CK, Vogel J. Small RNA-mediated activation of sugar phosphatase mRNA regulates glucose homeostasis. Cell. 2013; 153:426–437. [PubMed: 23582330]

Peer A, Margalit H. Evolutionary patterns of Escherichia coli small RNAs and their regulatory interactions. RNA. 2014; 20:994–1003. [PubMed: 24865611]

Pfeiffer V, Papenfort K, Lucchini S, Hinton J, Vogel J.r. Coding sequence targeting by MicC RNA reveals bacterial mRNA silencing downstream of translational initiation. Nature structural & molecular biology. 2009; 16:840–846.

Postma PW, Lengeler JW, Jacobson GR. Phosphoenolpyruvate:carbohydrate phosphotransferase systems of bacteria. Microbiol Rev. 1993; 57:543–594. [PubMed: 8246840]

Prasad C, Freese E. Cell lysis of Bacillus subtilis caused by intracellular accumulation of glucose-1-phosphate. J Bacteriol. 1974; 118:1111–1122. [PubMed: 4275311]

Prevost K, Salvail H, Desnoyers G, Jacques JF, Phaneuf E, Masse E. The small RNA RyhB activates the translation of shiA mRNA encoding a permease of shikimate, a compound involved in siderophore synthesis. Molecular microbiology. 2007; 64:1260–1273. [PubMed: 17542919]

Rehmsmeier M, Steffen P, Hochsmann M, Giegerich R. Fast and effective prediction of microRNA/target duplexes. RNA. 2004; 10:1507–1517. [PubMed: 15383676]

Rice JB, Balasubramanian D, Vanderpool CK. Small RNA binding-site multiplicity involved in translational regulation of a polycistronic mRNA. Proceedings of the National Academy of Sciences of the United States of America. 2012; 109:E2691–2698. [PubMed: 22988087]

Rice JB, Vanderpool CK. The small RNA SgrS controls sugar-phosphate accumulation by regulating multiple PTS genes. Nucleic Acids Res. 2011

Richards GR, Patel MV, Lloyd CR, Vanderpool CK. Depletion of glycolytic intermediates plays a key role in glucose-phosphate stress in Escherichia coli. J Bacteriol. 2013; 195:4816–4825. [PubMed: 23995640]

Richards GR, Vanderpool CK. Depletion of glycolytic intermediates plays a key role in glucose-phosphate stress in *Escherichia coli*. J Bacteriol. 2013; 195:4816–4825. [PubMed: 23995640]

Richter AS, Schleberger C, Backofen R, Steglich C. Seed-based INTARNA prediction combined with GFP-reporter system identifies mRNA targets of the small RNA Yfr1. Bioinformatics. 2010; 26:1–5. [PubMed: 19850757]

Robillard GT, Broos J. Structure/function studies on the bacterial carbohydrate transporters, enzymes II, of the phosphoenolpyruvate-dependent phosphotransferase system. Biochim Biophys Acta. 1999; 1422:73–104. [PubMed: 10393270]

Sharma CM, Darfeuille F, Plantinga TH, Vogel J. A small RNA regulates multiple ABC transporter mRNAs by targeting C/A-rich elements inside and upstream of ribosome-binding sites. Genes Dev. 2007; 21:2804–2817. [PubMed: 17974919]

Skippington E, Ragan MA. Evolutionary dynamics of small RNAs in 27 Escherichia coli and Shigella genomes. Genome Biol Evol. 2012; 4:330–345. [PubMed: 22223756]

Sledjeski DD, Whitman C, Zhang A. Hfq is necessary for regulation by the untranslated RNA DsrA. Journal of bacteriology. 2001; 183:1997–2005. [PubMed: 11222598]

Stim-Herndon KP, Flores TM, Bennett GN. Molecular characterization of adiY, a regulatory gene which affects expression of the biodegradative acid-induced arginine decarboxylase gene (adiA) of Escherichia coli. Microbiology. 1996; 142(Pt 5):1311–1320. [PubMed: 8704970]

Sun Y, Vanderpool CK. Regulation and function of Escherichia coli sugar efflux transporter A (SetA) during glucose-phosphate stress. J Bacteriol. 2011; 193:143–153. [PubMed: 20971900]

Sun Y, Vanderpool CK. Physiological consequences of multiple-target regulation by the small RNA SgrS in Escherichia coli. J Bacteriol. 2013; 195:4804–4815. [PubMed: 23873911]

Vanderpool CK, Gottesman S. Involvement of a novel transcriptional activator and small RNA in post-transcriptional regulation of the glucose phosphoenolpyruvate phosphotransferase system. Mol Microbiol. 2004; 54:1076–1089. [PubMed: 15522088]

Vanderpool CK, Gottesman S. The novel transcription factor SgrR coordinates the response to glucose-phosphate stress. J Bacteriol. 2007; 189:2238–2248. [PubMed: 17209026]

Wadler C, Vanderpool C. A dual function for a bacterial small RNA: SgrS performs base pairing-dependent regulation and encodes a functional polypeptide. Proceedings of the National Academy of Sciences of the United States of America. 2007; 104:20454–20459. [PubMed: 18042713]

Wadler C, Vanderpool C. Characterization of homologs of the small RNA SgrS reveals diversity in function. Nucleic acids research. 2009; 37:5477–5485. [PubMed: 19620214]

Wright PR, Richter AS, Papenfort K, Mann M, Vogel J, Hess WR, Backofen R, Georg J. Comparative genomics boosts target prediction for bacterial small RNAs. Proc Natl Acad Sci U S A. 2013; 110:E3487–3496. [PubMed: 23980183]

Yang Q, Figueroa-Bossi N, Bossi L. Translation enhancing ACA motifs and their silencing by a bacterial small regulatory RNA. PLoS Genet. 2014; 10:e1004026. [PubMed: 24391513]

Yarmolinsky MB, Wiesmeyer H, Kalckar HM, Jordan E. Hereditary Defects in Galactose Metabolism in Escherichia Coli Mutants, Ii. Galactose-Induced Sensitivity. Proceedings of the National Academy of Sciences of the United States of America. 1959; 45:1786–1791. [PubMed: 16590576]

Yu D, Ellis HM, Lee EC, Jenkins NA, Copeland NG, Court DL. An efficient recombination system for chromosome engineering in Escherichia coli. Proc Natl Acad Sci U S A. 2000; 97:5978–5983. [PubMed: 10811905]

Zhang A, Wassarman KM, Ortega J, Steven AC, Storz G. The Sm-like Hfq protein increases OxyS RNA interaction with target mRNAs. Molecular cell. 2002; 9:11–22. [PubMed: 11804582]

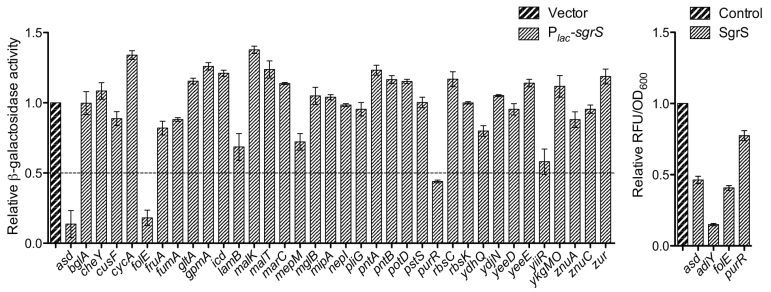

Figure 1. Post-transcriptional regulation of putative SgrS targets

A) Translational fusions to *lacZ* (controlled by P_{BAD} promoter) were constructed for the indicated genes. Reporter strains carrying vector or P_{lac}-*sgrS* plasmid were grown in TB medium with 0.002% L-arabinose to early exponential phase and 0.1 mM IPTG added to induce SgrS expression. β-galactosidase activity of the reporter fusion assayed at OD_{600}~0.5-0.6. Vertical dotted line indicates 2-fold change in expression. Error bars represent standard error for at least three independent biological replicates. B) *E. coli* carrying plasmids with P_{tet}-*sgrS* and target translational fusions to *gfp* reporter under the control of the P_{lac} promoter were cultured in MOPS rich medium with 0.2% fructose to mid-log phase. Relative fluorescence units (RFU) of GFP and optical density (OD_{600}) were measured. Activity in SgrS-expressing strains was normalized to activity in control strains. Error bars represent standard error for at least three biological replicates.

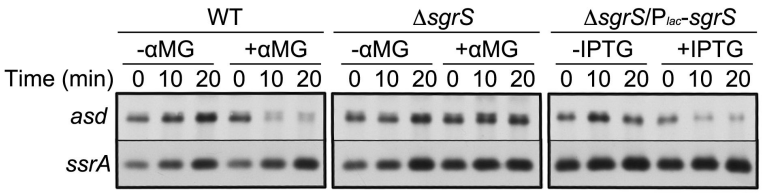

Figure 2. SgrS-dependent destabilization of *asd* mRNA during glucose phosphate stress response

E. coli strains Cp19-*asd* (MB4), Cp19-*asd* Δ*sgrS* (MB7) and Cp19-*asd* Δ*sgrS* with P_{lac}-*sgrS* plasmid (MB7 pLCV1) were grown in LB medium to OD~0.4. Total RNA was extracted at t=0, 10, 20 min. after addition of 0.5% αMG or 0.1 mM IPTG. Levels of *asd* mRNA were detected by northern blot.

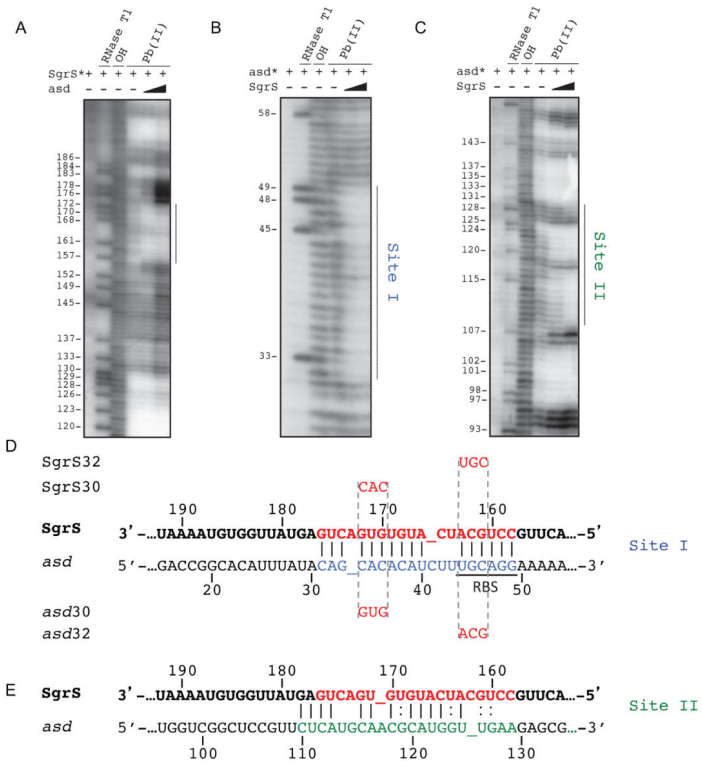

Figure 3. SgrS interacts with two distinct sites on *asd* mRNA

In vitro transcribed full length SgrS and *asd* mRNA fragments were generated using T7 RNA polymerase and labeled at the 5' end with ^{32}P radioisotope (*asd** and SgrS*). Labeled RNA was hybridized with unlabeled SgrS or *asd* as indicated, treated with RNase T1, alkaline hydrolysis (OH) or lead acetate (PbAc), and resolved on denaturing SDS PAGE. Positions of G residues are labeled. Footprint analysis indicates **A)***asd*-specific protection (lighter banding pattern) of SgrS, **B)** SgrS-specific protection in the *asd* mRNA leader (Site I) and **C)** SgrS-specific protection in the *asd* mRNA coding sequence (Site II). Representation of SgrS base pairing at two sites: **D)** *asd* mRNA leader (Site I) and **E)** *asd* mRNA coding sequence (Site II). Sequences highlighted in blue, green and red respectively correspond to Site I, Site II and *asd* protection observed in the footprinting experiments (A-C).

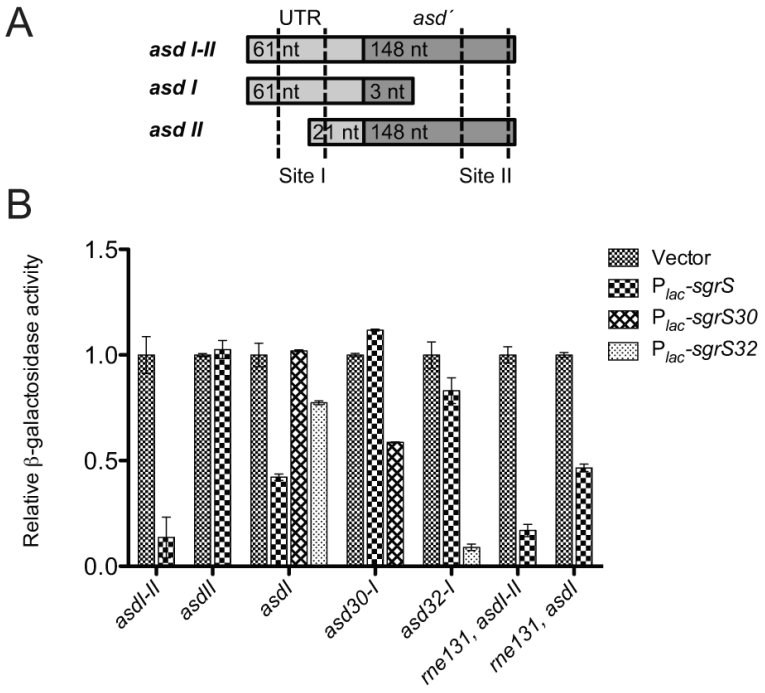

Figure 4. Characterization of SgrS base pairing with *asd* mRNA

A) Diagram of *asdI-II*, *asdI* and *asdII* with locations of SgrS binding Sites I and II B) β-galactosidase activity of translational *asdI-II-lacZ, asdI-lacZ* and *asdII-lacZ* reporter fusions was tested in the presence and absence of SgrS in wild-type and *rne131* hosts as indicated. Mutations in *asd* (*asd30-I, asd32-I*) disrupt complementarity with SgrS. Compensatory mutations in SgrS (SgrS30, SgrS32) restore complementarity.

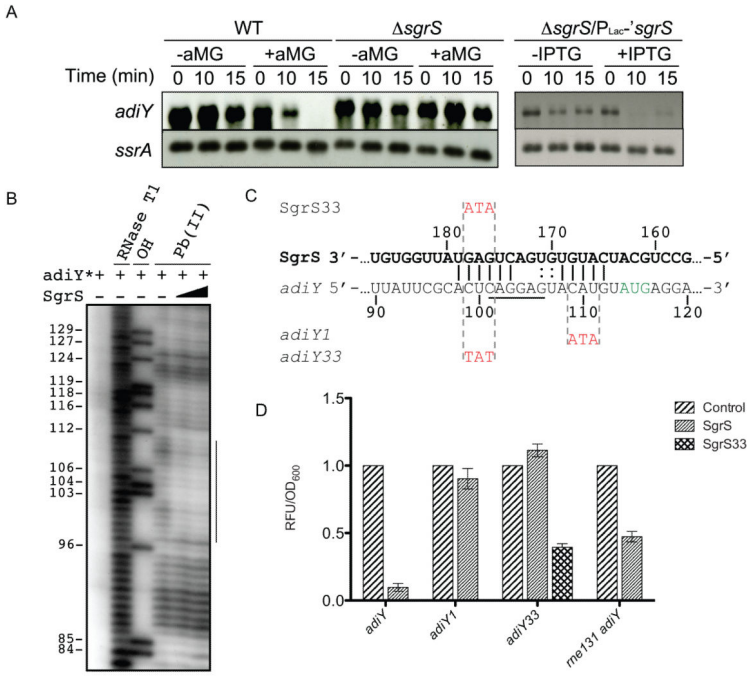

Figure 5. Characterization of post-transcriptional regulation of *adiY* by SgrS

A) *E. coli* strains Cp19-*adiY* (MB5), Cp19-*adiY* Δ*sgrS* (MB8) and Cp19-*adiY* Δ*sgrS*/P_{lac}-*sgrS* (MB8/pLCV1) (Table S2) were grown in LB to OD~0.4. RNA was extracted at 0, 5 and 15 minutes after addition of 0.5% αMG or 0.1 mM IPTG. *adiY* mRNA was detected by Northern blot. B) *In vitro* transcribed full length SgrS and *adiY* mRNA fragments were generated. 5′ end-labeled *adiY* mRNA (*adiY**) was hybridized with unlabeled SgrS where noted and treated with RNase T1, alkaline hydrolysis (OH) or lead acetate (Pb (II)), and resolved on denaturing SDS PAGE. Positions of G residues are indicated. C) Predicted base pairing of SgrS with *adiY* mRNA; *adiY1* and *adiY33* alleles contain mutations indicated in red; SgrS33 contains the indicated (red) compensatory mutation that restores complementarity to *adiY33*. Vertical lines represent predicted Watson-Crick (G:C, A:U) base-pairing and two dots represent non-canonical (G:U) interactions. D) *E. coli* Δ*sgrS* (JH111) and Δ*sgrS rne131* (MB12) strains carrying plasmids with P_{lac}-adiY'-'gfp (pZEMB18), P_{lac}-adiY1'-'gfp (pZEMB18-1) or P_{lac}-adiY33'-'gfp (pZEMB18-3) and P_{tet}-*sgrS* (pZAMB1) or P_{tet}-*sgrS33* (pZAMB1-4) were grown in rich MOPS medium with 0.2% fructose to exponential phase in the presence of the appropriate inducers. Relative fluorescence units (RFU) of GFP and optical density (OD_{600}) were measured. Activity in SgrS expressing strain was normalized to activity of the vector control strain. Error bars represent standard error for at least three biological replicates.

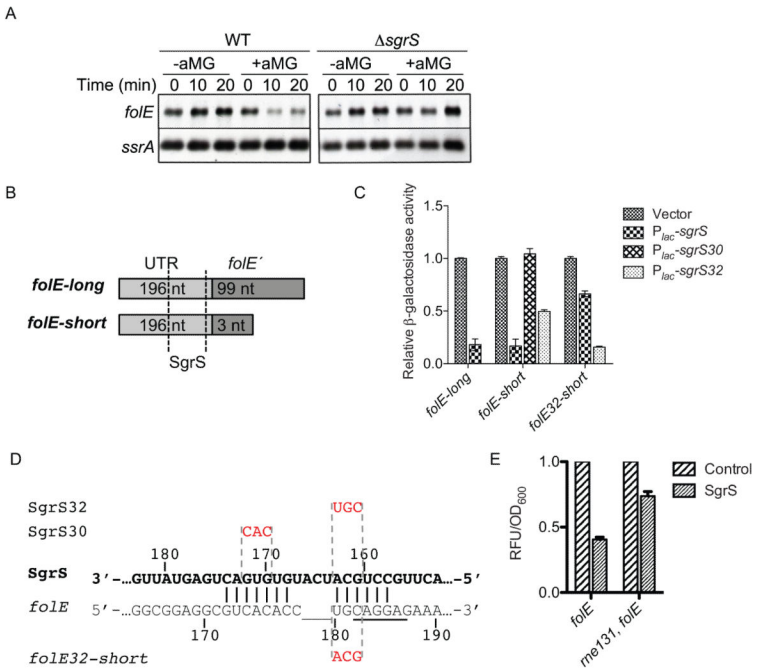

Figure 6. Characterization of post-transcriptional regulation of *folE* by SgrS

A) *E. coli* strains Cp19-*folE* (MB6) and Cp19-*folE* Δ*sgrS* (MB9) were cultured in LB medium to OD_{600}~0.4. Total RNA was extracted 0, 10, or 20 min. after addition of 0.5% αMG and *folE* mRNA detected by Northern blot. B) Truncated *folE* of different length used to construct *folE-long'-'lacZ* and *folE-short'-'lacZ* reporter fusions. C) β-galactosidase activity of translational *folE-long'-'lacZ* and *folE-short'-'lacZ* reporter fusions in the presence or absence of SgrS alleles. Fusion *folE32-short* contains mutations that restore complementarity with SgrS32 (shown in D). Error bars represent standard error for at least three biological replicates. D) Predicted SgrS-*folE* mRNA base pairing. Mutations corresponding to *folE32,* SgrS30 and SgrS32 are marked in red. The *folE* RBS is underlined. Vertical lines represent predicted Watson-Crick (G:C, A:U) base-pairing. E) *E. coli* Δ*sgrS* (JH111) and Δ*sgrS rne131* (MB12) with *folE'-'gfp* (pZEMB22) and vector control or P_{tet}-*sgrS* (pZAMB1) plasmids were grown in rich MOPS medium with 0.2% fructose to exponential phase in the presence of appropriate inducers. Relative fluorescence units (RFU) of GFP and optical density (OD_{600}) were measured. Activity in strains expressing SgrS was normalized to activity of the corresponding vector control strain. Error bars represent standard error for at least three biological replicates.

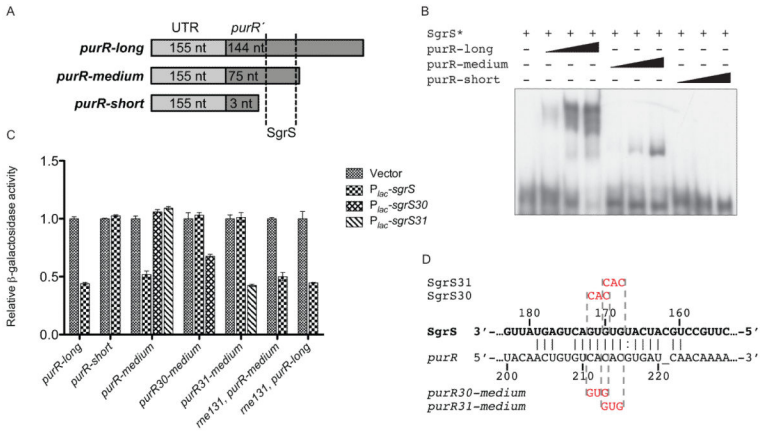

Figure 7. Characterization of post-transcriptional regulation of *purR* by SgrS

A) Limits of *purR* fragments that were used for gel shift assays (B) and translational fusions (C). B) Full length SgrS and truncated *purR* transcripts were synthesized in vitro. 5′-end labeled SgrS (SgrS*) and increasing concentrations of unlabeled *purR-short, purR-medium* and *purR-long* RNAs were hybridized and resolved on native PAGE. C) β-galactosidase activity of indicated *purR* translational reporter fusions was tested in the absence or presence of SgrS alleles. The sequences of wild-type and mutant SgrS and *purR* are indicated in D. Compensatory mutations *purR30* and *purR31* restore base pairing with SgrS30 and SgrS31 mutants, respectively. Error bars represent standard error for at least three biological replicates. D) Predicted SgrS-*purR* mRNA base pairing interactions. Mutations corresponding to *purR30*, *purR31* and SgrS30, SgrS31 are indicated in red. Vertical lines represent predicted Watson-Crick (G:C, A:U) base pairing and two dots represent noncanonical (G:U) interactions.

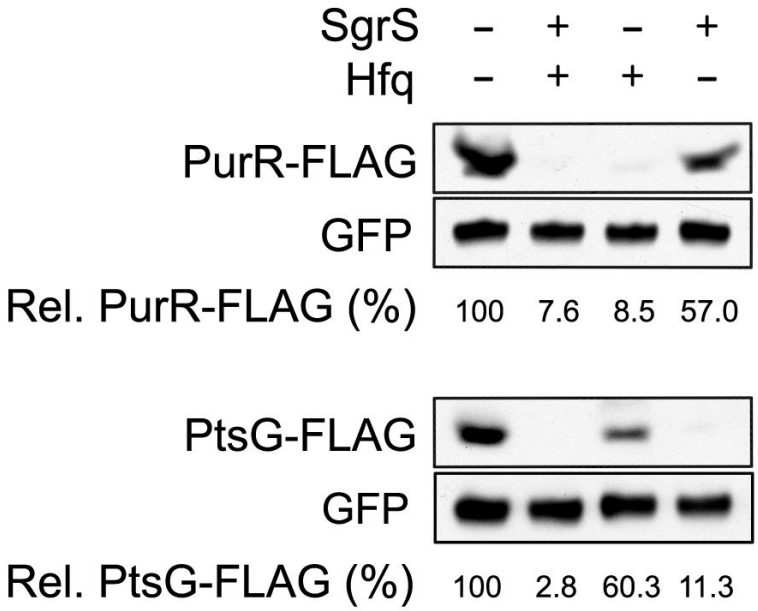

Figure 8. Inhibition of *purR* translation by SgrS

In vitro transcription generated *purR*-3xFLAG, *ptsG*-3xFLAG, *gfp* and SgrS RNAs. *purR* and *ptsG* RNAs were mixed with SgrS in the presence or absence of Hfq and *in vitro* translation was performed. Control *gfp* RNA was supplemented in each reaction. Products of translation were detected by Western blot with anti-FLAG or anti-GFP antibodies. Bend densities were measured using ImageJ and normalized to GFP controls.

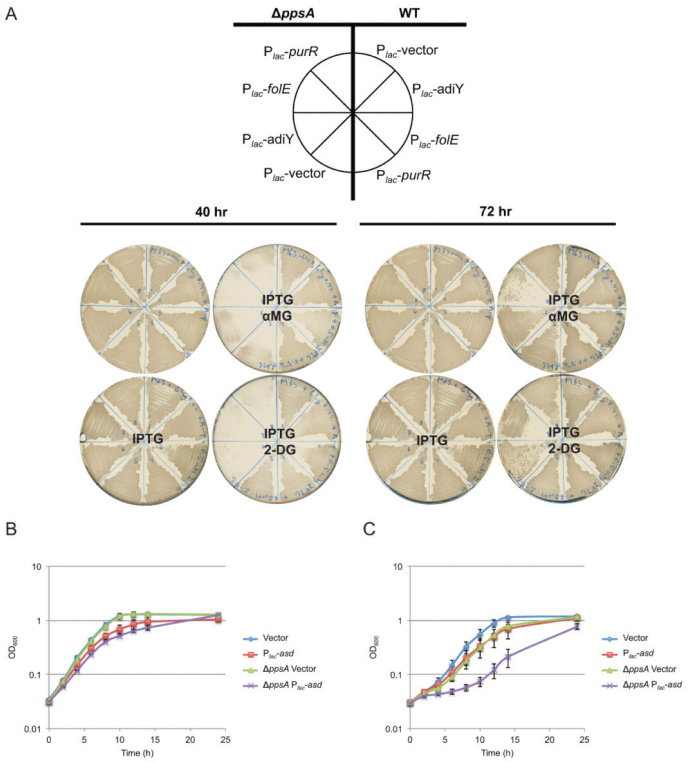

Figure 9. Target overexpression phenotypes in stressed *E. coli* cells

A) *E. coli* wild-type and Δ*ppsA* mutant strains harboring P*lac-adiY,* P*lac-folE,* P*lac-purR* plasmids or vector control were cultured on M63 minimal plates with 0.4% glycerol and combinations of IPTG, αMG or 2DG as indicated. Growth was observed after 40 and 72 hours of incubation. B,C) *E. coli* WT and Δ*ppsA::kan* strains ectopically expressing *asd* (or with vector control) were grown in minimal fructose medium in the C) presence of 0.5% αMG and B) absence of the stressor.

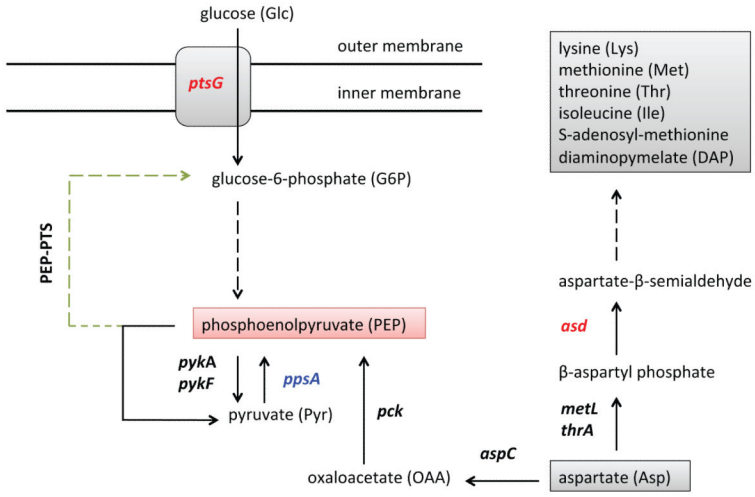

Figure 10. Relevant pathways of carbon utilization in *E. coli*

Glucose and its analogs are taken up by the cell through the phosphotranferase system (PTS) that relays a phosphate group from phosphoenolpyruvate (PEP) to the incoming sugar during translocation. Glucose-phosphate then enters glycolysis to replenish the pool of PEP that was diminished during the uptake process. Block in glycolysis or uptake of non-metabolizable glucose analogs results in accumulation of these phosphosugars in the cytoplasm and inability to replenish PEP through glycolytic flux. Under such conditions, PEP can be produced from pyruvate or oxaloacetate (OAA) through the action of enzymes encoded by *ppsA* (in blue) and *pck* genes respectively. While aspartate can be utilized to produce OAA, aspartate semialdehyde dehydrogenase encoded by *asd* (in red) is essential in aspartate utilization pathway producing other amino acids.

Table 1
Differential gene expression after SgrS pulse expression

E. coli CV104 (Δ*sgrS*) carrying vector or P_{lac}-*sgrS* plasmid was grown in defined MOPS rich medium with 0.2% glucose to OD_{600}~0.5. Total RNA was extracted 10 minutes after addition of 0.1 mM IPTG. RNA-seq was performed and data analyzed using Rockhopper (McClure *et al.*, 2013). Genes with ≥1.5-fold change in expression (P_{lac}-*sgrS*/vector) and statistical significance of $<1\times10^{-2}$ (qValue) are shown. Increase in expression is indicated by fold-change >1 and decrease in expression is indicated by fold-change <1. Post-transcriptional regulation is characterized as translationally activated (Act), translationally repressed (Rep), not regulated (NR).

Gene Name	Product Description	Fold-change P_{lac}-*sgrS*/vector	qValue	Post-transcriptional Regulation
sgrT	inhibitor of glucose uptake	215.00	0	
sgrS	sRNA regulator of glucose-phosphate stress response	191.68	0	
zinT	zinc and cadmium binding protein, periplasmic	15.88	0	NR
cusF	periplasmic copper- and silver-binding protein	0.08	0	NR
ptsG	fused glucose-specific PTS enzymes: IIB component/IIC component	0.07	0	Rep
cusC	copper/silver efflux system, outer membrane component	0.01	0	
ykgM	rpmE (L31) paralog	4.58	9.77E-163	NR
ykgO	rpmJ (L36) paralog	3.90	2.37E-113	NR
znuA	zinc transporter subunit: periplasmic-binding component of ABC superfamily	3.80	1.10E-70	NR
yebA	predicted peptidase	2.47	1.17E-27	NR
yeiB	predicted inner membrane protein (in operon with *folE*)	0.51	3.78E-17	
pliG	predicted protein	2.25	1.85E-16	NR
asd	aspartate-semialdehyde dehydrogenase, NAD(P)-binding	0.51	2.54E-15	Rep
purR	DNA-binding transcriptional repressor, hypoxanthine-binding	0.54	2.77E-12	Rep
yeeD	conserved protein (in operon with *yeeE*)	0.58	2.97E-11	NR
manX	fused mannose-specific PTS enzymes: IIA component/IIB component	0.60	9.89E-10	Rep
znuB	zinc transporter subunit: membrane component of ABC superfamily	2.05	1.43E-09	
yigL	sugar phosphatase	1.77	9.19E-09	Act
znuC	zinc transporter subunit: ATP-binding component of ABC superfamily	1.86	1.47E-07	NR

Gene Name	Product Description	Fold-change P_{lac}-*sgrS*/vector	qValue	Post-transcriptional Regulation
folE	GTP cyclohydrolase I	0.54	7.25E-07	Rep
ydjN	predicted transporter	0.56	2.25E-06	NR
malK	fused maltose transport subunit, ATP-binding component of ABC superfamily	1.57	1.41E-04	NR
mglB	methyl-galactoside transporter subunit	1.62	2.48E-03	NR